scientific reports

Check for updates

OPEN

Uncovering the influence of gold tailings on foam stability and mechanical performances of foamed concrete

Xinyu Wang[1], Yuanliang Xiong[1], Chunfei Zhang[2], Yuanjing Wang[3], Bo Liu[1]✉ & Yuming Liu[4]

The present investigation is dedicated to exploring the potential of utilizing gold tailings to enhance the performances of foam concrete. Tests to assess foam stability and compressive strength have been performed. The inherent yield stress exhibited by the matrix is utilized as a metric to evaluate the foam stability of the foamed concrete. Compressive strength of matrix and density ratio are employed to analyze and predict the strength of foam concrete. The experimental findings unveil that mechanical performances of foam concrete can be augmented through the incorporation of an optimal quantity of gold tailings. This enhancement can be attributed to the development of a more compact and less permeable microstructure. However, it should be noted that the inclusion of gold tailings may also have an adverse effect on the foam stability of foamed concrete. This is due to their ability to enhance the fluidity and decrease the yield stress of the base mix, thereby reducing the overall stability of the foam concrete. The main control factors of foam concrete strength are determined by using the prediction model. Compared with the foam stability, the enhancement in compressive strength of base mix, coupled with a consistent density ratio may account for the enhancement of compressive strength in foam concrete.

Keywords Foamed concrete, Gold tailings, Pore structure, Compressive strength

Foam concrete, a porous substance that has garnered considerable acclaim across multiple industries, has emerged as a material of great interest. This heterogeneous and lightweight substance is created by infusing bubbles into the paste of cement or mortar. Such a distinctive composition imparts several coveted characteristics to foam concrete, including exceptional thermal insulation, remarkable fluidity, notable porosity, and decreased density[1–3]. With such exceptional qualities, foam concrete finds itself well-suited for a myriad of applications, insulation components and even road infrastructure. Its versatility knows no bounds, as it seamlessly integrates into various domains, offering unmatched performance and unparalleled benefits. Furthermore, it has demonstrated its efficacy in the fabrication of adsorbent materials, photocatalysts, and as an integral element in the realm of additive manufacturing[4–6]. Nevertheless, notwithstanding its myriad benefits, foam concrete is besieged by inherent limitations including inadequate stability, moderate compressive potency, and pronounced vulnerability to volumetric contraction.

Gold tailings (GT), the residual byproduct left in the wake of gold ore extraction and separation[7], represent a prominent subset of tailings in the China. Regrettably, in the year 2018 of China, the utilization efficiency of gold tailings remained at a meager 36.9%[8]. A copious volume of these gold tailings currently reside in vast repositories, known as tailings ponds, which not only encroach upon precious land resources but also engender deleterious repercussions upon the environment and water reservoirs[9,10]. To address this conundrum, a cohort of scholars has ventured into exploring the potential of employing tailings as efficacious fillers[11,12] and construction materials[13–18] for disposal purposes. As an illustrative example, in a groundbreaking study conducted by Alieh et al.[19], the latent potential of zinc tailings came to fruition as a substitute for cement in concrete production. The findings of their research showcased the remarkable capabilities of this innovative approach, with the concrete demonstrating an unparalleled 28-day compressive strength. Remarkably, when 20% of the cement was substituted with zinc tailings, the 28-day compressive strength experienced a noteworthy augmentation of 5.23 MPa, stunning results that surpassed those of the control group. Moreover, the groundbreaking work of Çelik

[1]School of Civil Engineering, Yantai University, Yantai 264005, China. [2]China Communications Construction (Nanjing) Co., Ltd, Nanjing 211189, China. [3]Lunan High Speed Railway Co., Ltd, Jinan 250000, China. [4]Yantai Feilong Group Co., Ltd, Yantai 264005, China. ✉email: liuboYTU6280@163.com

et al.[20] illuminated the feasibility of using gold tailings as an active ingredient to produce the Portland cement, with a recommended content of 25%. This remarkable finding opens up new avenues for the reutilization of gold tailings in cementitious materials. In addition, successful applications of gold tailings in fiber-reinforced concrete have been documented. Tanvir Ahmed et al.[21] explored the utilization of gold tailings to replace quartz sand in the preparation of UHPC, and they achieved satisfying results with a substitution rate of 80%, showcasing the immense potential of gold tailings in pushing the boundaries of concrete strength. The utilization of gold tailings in the preparation of foam concrete as a filling material holds momentous significance in facilitating the large-scale application of gold tailings, thereby harboring expansive prospects for development and implementation. Liang et al.[22] carry out the compressive strength, and pore structure of foam concrete including gold tailings. However, the impact of gold tailings on foam stability and compressive strength of foamed concrete and its action mechanisms need to be further clarified.

In this study, the utilization of gold tailings serves as the basis for the production of foamed concrete. An in-depth exploration is undertaken to gauge the foam stability and mechanical attributes. The measurement of yield stress is conducted and subsequently linked to the foam stability and pore sphericity inherent in the foamed concrete. Moreover, the assessment of the mechanical properties is carried out through a meticulous analysis of its microstructures.

Materials and methods

Materials and mixing proportions

The production of foamed concrete entailed the utilization of ordinary Portland cement (OP) of P.O. 42.5 grade with density of 2.90, S95 grade ground granulated blast furnace slag (GBFS) with density of 2.88 g/cm^3, and gold tailings (GT) with density of 2.74 g/cm^3. The precise chemical composition of OP, GGBS, and GT is meticulously delineated in Table 1, providing a comprehensive overview of their elemental constituents. To serve as an alkaline activator, calcium hydroxide were employed. Furthermore, the foam was generated through the use of a synthetic surfactant modified with nano-Al_2O_3, as elucidated in previous studies[23–25]. The XRD patterns of OP, GBFS and GT are shown in Fig. 1.

Preparation of foamed concrete

The precise ratios for the blending of the foamed concrete to achieve a desired density are meticulously explicated in Table 2. The initial step involved the introduction of $Ca(OH)_2$ into the water. In order to generate the foam, the synthetic surfactant, enhanced with nano-Al2O3, was meticulously dissolved in water at a ratio of 1:300. The mixture of OP, GGBS, and GT was blended for a duration of 30 s to ensure a homogeneous consistency. Subsequently, this arid amalgamation was meticulously dissolved in water infused with $Ca(OH)_2$, culminating in a harmonious paste. Ultimately, the ethereal foam was introduced into the paste, thereby begetting a pristine and lustrous concoction of foam concrete.

Test methods

Settlement

The settlement of the foamed concrete was painstakingly evaluated through the implementation of a remarkably accurate laser displacement sensor (JINGJIAKE BX-LV30), guided by the authoritative references[26,27]. By observing the settlement of the fresh foamed concrete, the depth of defoaming can be accurately determined, allowing for the evaluation of foam stability. The settlement measurements of both the concrete matrix and the fresh foamed concrete were recorded.

Yield stress measurement

In order to scrutinize the yield stress of the concrete matrix, the mini cone test was embraced as the preferred experimental approach[28].

XRD analysis

To analyze the phases present in the samples, the X-ray diffraction (XRD) scanning was performed over a range of 5 to 70°, with a scanning speed of 0.02°per step[29]. For the XRD test, the samples were prepared along with an internal standard substance of 10 wt% α-Al_2O_3[30,31].

Microstructure, bubble evolution, and pore structures of foamed concrete

To examine the microstructure of the foamed concrete, the SEM-EDS technique was utilized.

To investigate the progressive development of bubbles, the utilization of the photon microscope (RY605) was used to facilitate the microscopic analysis.

Furthermore, the pore size of foamed concrete was assessed using the optical microscope (RY605). For this analysis, specimens with dimensions of ϕ 30 mm×30 mm, carefully extracted from the center of the ϕ 30 mm

Type	CaO	SiO_2	Al_2O_3	Fe_2O_3	MgO	SO_3	K_2O	Na_2O	LOI
Cement	51.42	24.99	8.26	4.03	3.71	2.51	0.65	0.11	4.32
GBFS	35.58	35.10	16.32	0.69	9.32	1.17	0.41	0.49	0.92
GT	11.19	60.16	13.22	4.83	2.29	0.48	1.27	4.11	2.45

Table 1. Compositions of OP, GBFS, GT wt%.

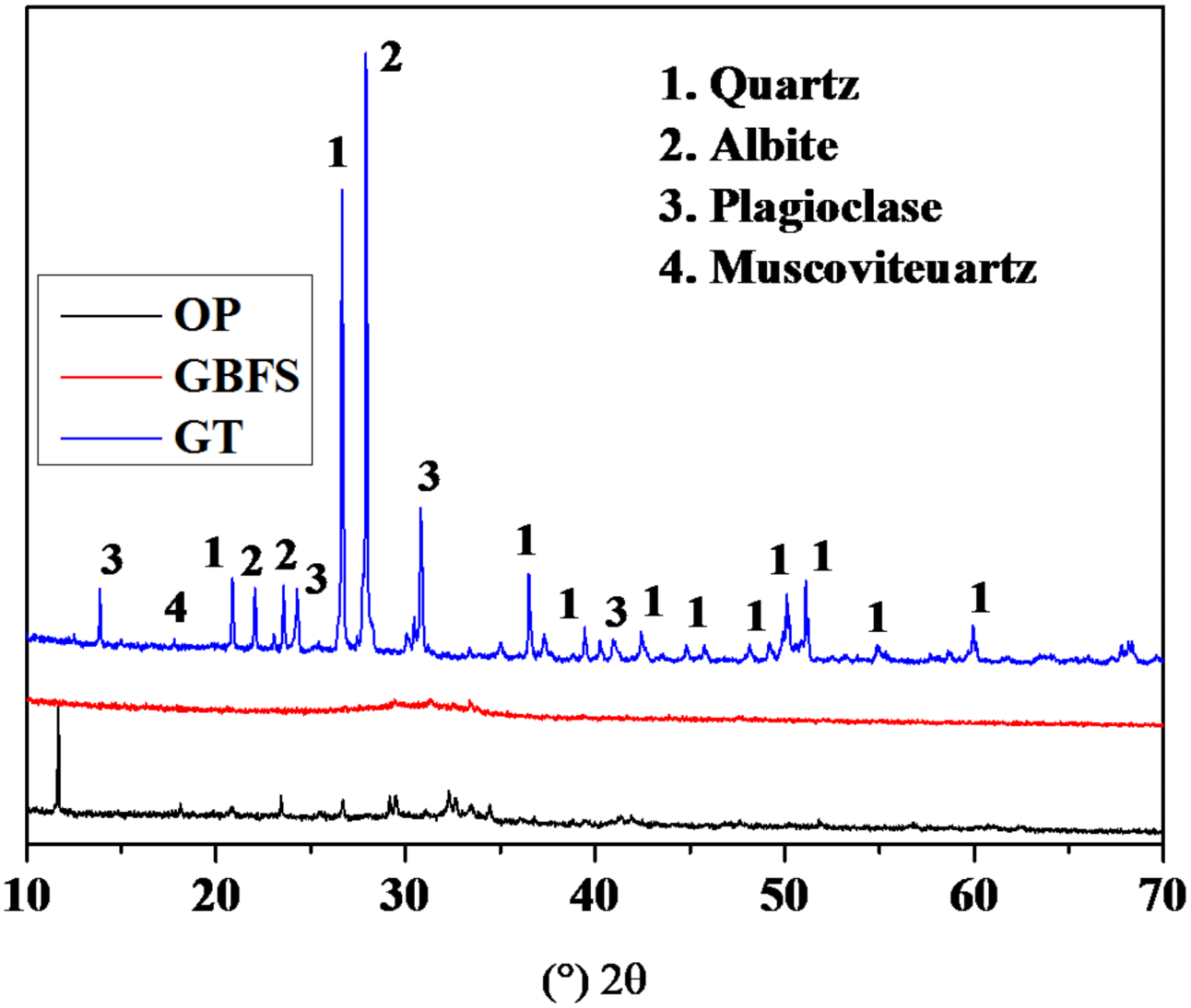

Fig. 1. XRD results of OP, GBFS and GT.

Mix	Target density (kg/m^3)	OP (kg)	GBFS (kg)	GT (kg)	Water (kg)	CaOH (%)	Actual foam (m^3)	Dry density (kg/m^3)
FC-REF	600	75	299	-	187	5	0.9	626 ± 3
FC-GT-5%	600	75	261.6	37.4	187	5	0.9	623 ± 5
FC-GT-10%	600	75	224.2	74.8	187	5	0.9	617 ± 4
FC-GT-20%	600	75	186.8	112.2	187	5	0.9	612 ± 4

Table 2. Mix proportions of foamed concrete.

cylinder with the heights of 300 mm, were meticulously chosen. These ϕ 30 mm×30 mm specimens underwent a meticulous preparation process, involving polishing with fine grinding papers of 2000 mesh and subsequent cleaning with acetone.

Compressive strength

To evaluate the compressive strength of the base mix and foamed concrete, samples with size of 70.7 mm×70.7 mm×70.7 mm were carefully prepared and cured under controlled conditions of 20 ± 2℃ and 95 ± 2% relative humidity. Before conducting the compressive strength test, these specimens underwent a meticulous drying process at a temperature of 60℃. In order to obtain a reliable average value, three samples were utilized for each measurement of compressive strength. The compressive strength test was conducted at a loading speed of 1kN/s.

Results and discussion

Settlement and compressive strength of foamed concrete

Figure 2 shows the settlement of fresh foamed concrete, wherein the settlement values at the 90-minute mark for FC-REF, FC-GT-5%, FC-GT-10%, and FC-GT-20% are 0.935 mm, 2.238 mm, 2.947 mm, and 3.161 mm. It is apparent that with an increasing dosage of GT, the settlement of fresh foamed concrete also exhibits a corresponding increase. However, it is noteworthy that the settlement rate gradually decreases, indicating an improvement in the stability of the foamed concrete. This phenomenon may be owing to the formation of interstitial paste, which provides resistance against destabilizing forces acting on the bubbles, as previously highlighted in studies[32,33]. The observed phenomenon can be attributed to various factors, including the yield stress, which will be further examined in section "Pore size of foamed concrete ".

Figure 3 illustrates compressive strength variations of the foam concrete with varying dosages of GT. The compressive strength of the FC-REF, FC-GT-5%, FC-GT-10%, and FC-GT-20% is 1.87 MPa, 2.02 MPa, 2.19 MPa, and 1.70 MPa. With the augmentation of GT dosage, the compressive strength of foam concrete demonstrates an initial upsurge, subsequently followed by a subsequent decline. Contrary to findings in existing literature[24,26], this study reveals an unconventional relationship between stability and strength in foamed concrete. Typically, a higher level of stability would correspond to greater strength. However, intriguingly, the results of this study demonstrate that foamed concrete with lower stability exhibits higher strength. The underlying causes of this anomalous phenomenon will be thoroughly investigated in section "Compressive strength changes law and its prediction".

Influence of gold tailings on foam stability of foamed concrete

Table 3 displays the flow spread measurements alongside their respective yield stress values, which exhibit variability across different precursors. Notably, an escalation in GT dosage yields a diminished rate of spread loss, consequently mitigating the progression of yield stress. These discoveries establish a cohesive correlation between the stability of foamed concrete and the progression of yield stress.

Within the spectrum of foam collapse mechanisms, coarsening and coalescence engender the expansion of bubbles, consequently precipitating bubble rearrangement. Bubbles adorned with denser walls exhibit a

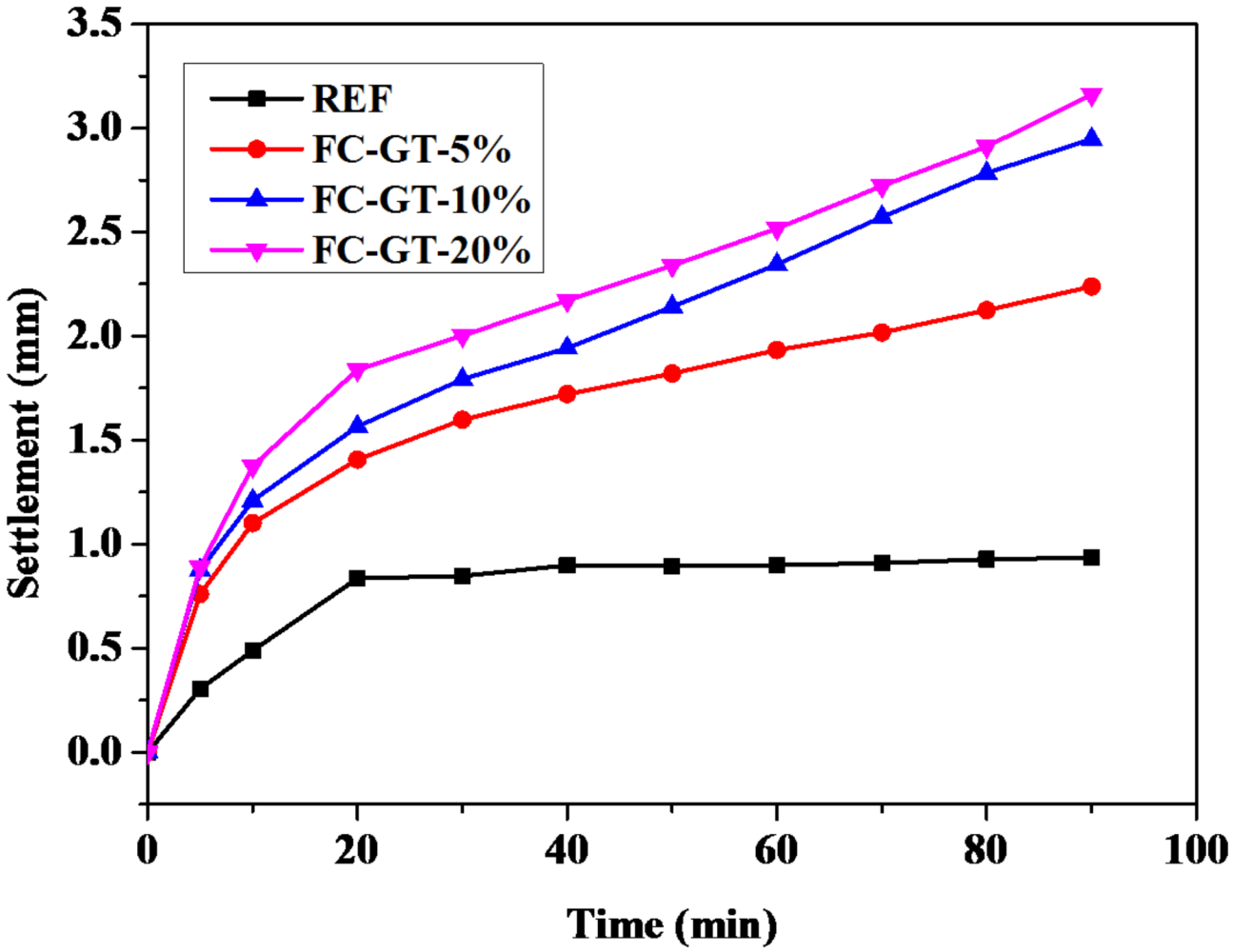

Fig. 2. Settlement of fresh foamed concrete.

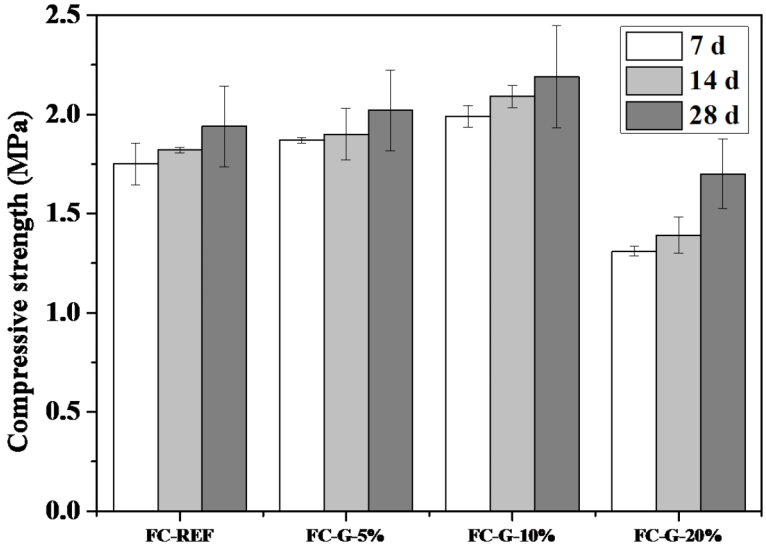

Fig. 3. Compressive strength of foam concrete with various precursors.

Mix	Spread (mm)			Yield stress (Pa)		
	0 min	30 min	60 min	0 min	30 min	60 min
BM-REF	150	142	132	10.34	21.14	50.54
BM-GT-5%	173	162	154	8.07	20.95	39.05
BM-GT-10%	196	185	175	7.53	16.49	36.49
BM-GT-20%	233	217	201	5.27	13.61	24.94

Table 3. Fluid propagation and the yield stress.

diminished propensity for maturation and fusion. Diminishes the thickness of bubble walls, thereby facilitating the collapse of bubbles through the exquisite dance of coalescence and the graceful maturation process, as if in a mesmerizing performance[26]. As a result, the investigation delves into the collapse of freshly prepared foamed concrete induced by drainage.

The exquisite phenomenon of foam drainage manifests as a mesmerizing dance, where the fluid gracefully permeates through the intricate porous medium. However, this ethereal flow encounters a formidable obstacle when the yield stress of the matrix (τ) surpasses the eminent threshold of the critical yield stress (τ_0). The determination of τ_0 for the foam can be achieved through the utilization of Eq. (1)[34].

$$\tau_0 \cong \rho_1 g r \tag{1}$$

whereτ_0 denotes the critical yield stress of foam, ρ_1 signifies the density of the fluid, g represents the gravitational acceleration, and r denotes the dimensions of the pore radius.

Within the realm of foam, the parameter "r" can be interpreted as the utmost extent of the pore radius, bestowing it with the capacity to facilitate the graceful flow of fluid within the intricate porous medium. This radius, denoted as "r" is ascertained by employing the bubble radius, symbolized by "R" in conjunction with the foam volume fraction, represented by the elegant symbol "ϕ" as expounded in Eq. (2)[35].

$$r = R\frac{0.27\sqrt{1-\phi} + 3.17(1-\phi)^{2.75}}{1 + 0.57(1-\phi)^{0.27}} \tag{2}$$

The foam volume fraction, ϕ, is displayed in Table 2, while the progression of bubble evolution at 0 min, 60 min, and 90 min is visually captured in Fig. 4. The exquisite characterization of the bubble diameter distribution in newly formed foamed concrete, obtained through the utilization of various precursors and analyzed using Image Pro Software, is showcased in Fig. 5. It should be noted that the yield stress fluid tends to experience drainage with an increased bubble diameter. Therefore, the pivotal threshold of yield stress, denoted as τ_0, is computed by taking into account the utmost bubble radius of 50 μm. By employing the values $R \approx 50\ \mu$m, $\phi = 90\%$, Eqs. (1) and (2) enable the determination of r and τ_0. The resulting calculation yields a τ_0 value of 0.15 Pa.

The value of τ significantly surpasses τ_0, signifying that the foam drainage in newly formed foamed concrete is effectively averted. The occurrence of bubble coarsening within the matrix can potentially contribute to

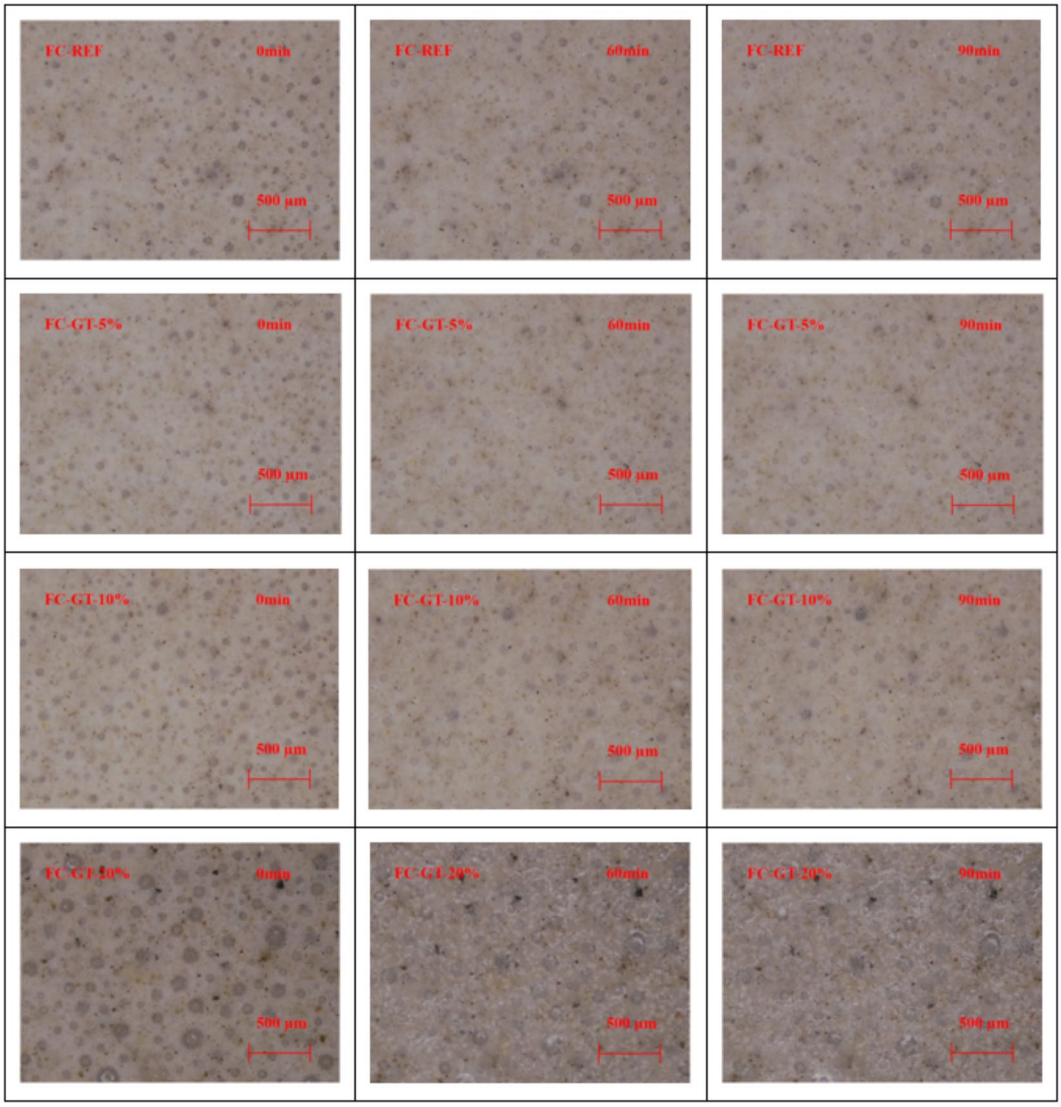

Fig. 4. The process of bubble evolution in freshly foamed concrete (HAAFC) with different precursor materials (**a**) FC-REF, (**b**) FC-GT-5%, (**c**) FC-GT-10%, (e) FC-GT-20%.

the buoyancy of the bubbles, consequently resulting in the deaeration of fresh foam concrete. This concept is illustrated in a conceptual diagram illustrating the forces exerted upon an individual bubble[36]. Additionally, it is observed that the yield stress of foamed concrete diminishes with an increase in GT dosage. Consequently, the restraining force exerted by the basal body on the bubbles is prone to undergo a decrease, owing to the decrease in yield stress. As a result, the foam stability of foamed concrete exhibits a propensity to decrease with a corresponding increase in GT dosage.

During the initial phase, notable variations in bubble pore size at the same level of magnification are observed. However, after a continuous in-situ observation period of 90 min, the various groups of bubbles gradually transform into pores. By the 90-minute mark, the FC-REF, FC-GT-5%, and FC-GT-10% samples exhibit a progressive development of preliminary pore morphology, while the FC-GT-20% sample has already formed discernible pore structures. Notably, the presence of GT appears to facilitate the formation of a more expansive and less compact pore structure in the foamed concrete. These pores, present in all the groups, exhibit a relatively independent nature, with thick pore walls. The association between the looser pore structure observed in foamed concrete containing GT and the lower yield stress prior to foam addition is evident.

Pore size of foamed concrete

Figure 6 illustrates the two-dimensional depictions of foamed concrete incorporating diverse precursor materials, while the analysis of pore sizes was conducted utilizing the sophisticated Image Pro Plus software. The pore size and its distribution of the foamed concrete samples are illustrated in Fig. 7. It is evident that the percentage of pores with a diameter ranging from 100 μm to 200 μm in the FC-REF, FC-GT-5%, FC-GT-10%, and FC-GT-20% samples are 41.49%, 36.00%, 33.03%, and 22.40%, respectively. Significantly, an escalation

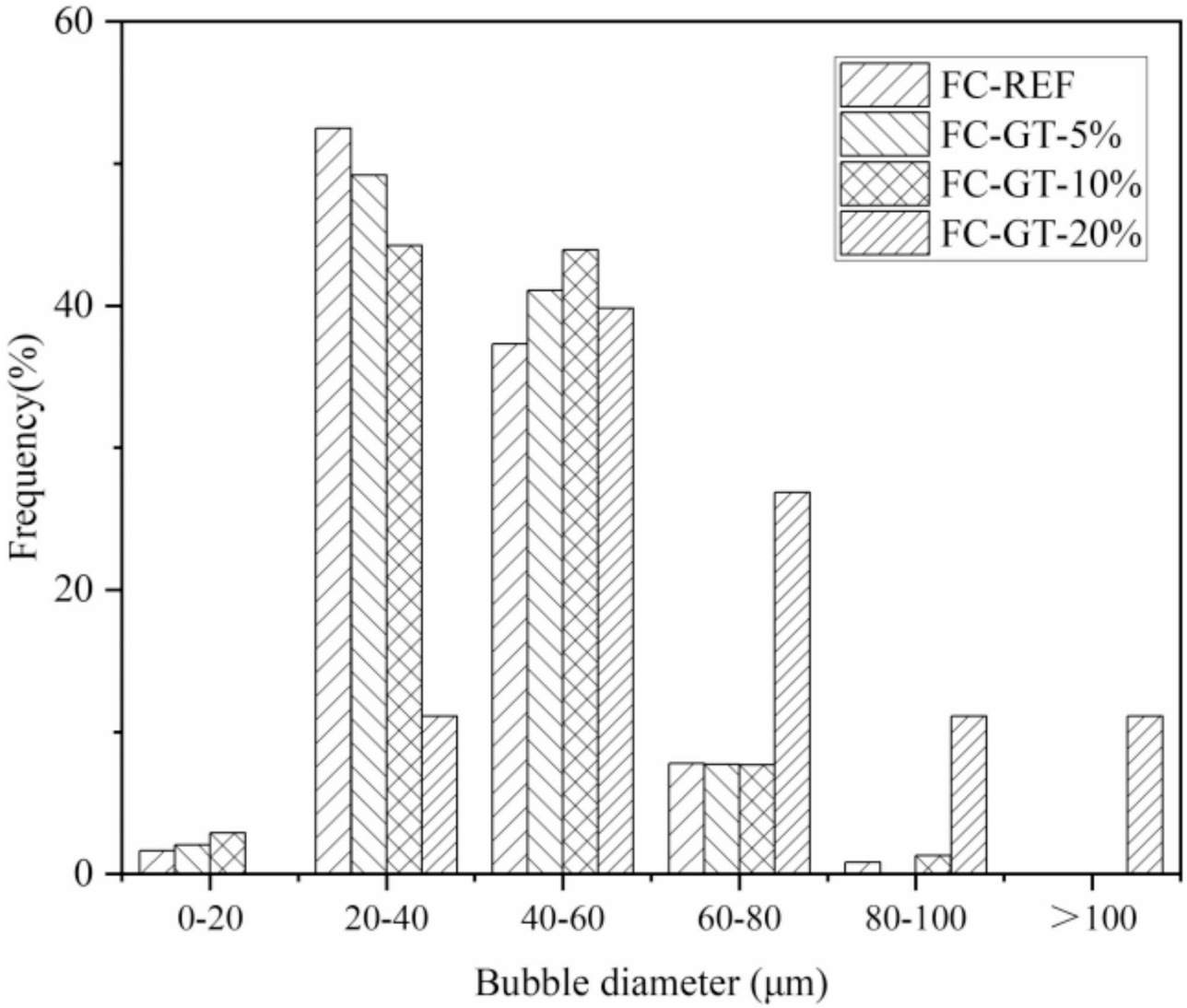

Fig. 5. The spatial arrangement of bubbles in freshly mixed foamed concrete with different precursor materials (t = 0).

in GT dosage is correlated with an increase in small-sized pores, suggesting that The inclusion of GT in the composition of foamed concrete fosters the formation of larger pore structures. Notably, the foamed concrete incorporating GT exhibits a more expansive pore structure, potentially attributable to the reduced foam stability in fresh foamed concrete.

Compressive strength changes law and its prediction

Figure 8 exhibits the compressive strength of matrix utilizing various precursors. Yaseen et al.[37] unveiled a method to evaluate the compressive strength of matrix (f_{cc}) by leveraging the compressive strength of foamed concrete (f_c) and air content (A). This innovative approach is elegantly encapsulated in Eq. (3), offering a profound insight into the interconnectedness of material properties and the potential for predictive modeling in the realm of hybrid alkali-activated materials.

$$fcc = 1.048 f_c (1 - A)^{2.793} \tag{3}$$

In a groundbreaking contribution, Kearsley and Wainwright[38] put forth a visionary perspective on the estimation of compressive strength in foamed concrete. They proposed an ingenious formula, elegantly expressed in Eq. (4), which hinges on the utilization of the binder ratio (α_b) (expressed in terms of volume). This pioneering methodology opens up new avenues for accurately anticipating the impending compressive strength of foamed concrete through a meticulous analysis of key parameter inputs, further enhancing our understanding of this remarkable material.

$$f_{cc} = 1.172 f_c \alpha_b^{3.7} \tag{4}$$

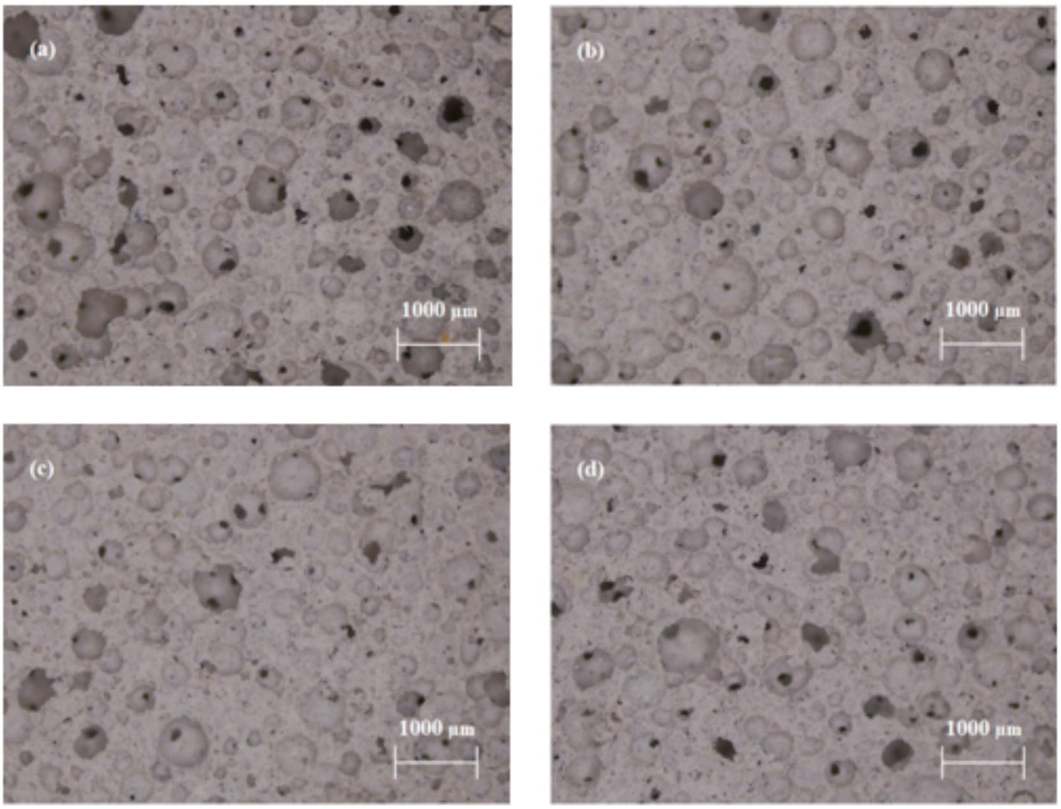

Fig. 6. Two-dimensional renditions capturing the essence of foamed concrete. (**a**) FC-REF, (**b**) FC-GT-5%, (**c**) FC-GT-10%, (**d**) FC-GT-20%.

In a groundbreaking study, Kearsley and Wainwright[38] made a remarkable observation: as the density of foam concrete decreases, the disparities between the experimental and computed outcomes of compressive strength. This intriguing finding suggests that the compressive strength is intricately interwoven with the intricate properties of its pores, encompassing factors such as the distribution and overall volume of these minuscule voids. To incorporate these pore features into the calculation, they introduced the notion of a density ratio (α_d), which elegantly captures the relationship between the arid density of foamed concrete and the arid density of its matrix. Leveraging insights from reference[39], they devised Eq. (5) as an elegant means to estimate the compressive strength, taking into account the impact of pore features. This novel approach further advances our understanding of the complex interplay between density, pore characteristics, and compressive strength in foamed concrete systems.

$$f_{cc} = f_c(-0.324 + 1.325\alpha_d)^2 \tag{5}$$

The comparison of calculated and experimental compressive strength values is outlined in Table 4. It is noteworthy that the relative discrepancy between the empirical and computed outcomes lies within a modest 10%, thus accentuating the dependability in prognosticating the compressive potency of foamed concrete via the amalgamation of its compressive strength (f_c) and the density ratio (α_d). Furthermore, in line with findings from reference[40], the escalation of GT dosage corresponds to a reduce in the compressive strength of the base mix. This observed enhancement in compressive strength of base mix, coupled with a consistent density ratio, provides a compelling explanation for the increased compressive strength of the foamed concrete, as stipulated by Eq. (5).

Microstructure and XRD analysis

Figure 9 showcases the magnified microstructures of foam concrete, observed through Scanning Electron Microscopy (SEM) at a magnification of 100x. As the cement dosage increases, there is an initial decline in the presence of defects within the matrix, followed by a subsequent escalation. The defects and loose pore walls can be observed in the SEM microstructures of FC-REF, and FC-GT-5%. The denser and less porous microstructure of foamed concrete can be observed in FC-GT-10% group. The more pores and cracks could be observed in FC-GT-20% group, indicating that the appropriate amount of gold tailings can effectively improve the compactness of foam concrete pore walls, however, excessive gold tailings will introduce cracks and other defects in the pore wall of foam concrete.

The XRD patterns of foamed concrete are shown in Fig. 10. The CH, C-S-H, and C-A-S-H gels can be observed in Fig. 10. Additionally, the internal driving force responsible for promoting strength development is generated.

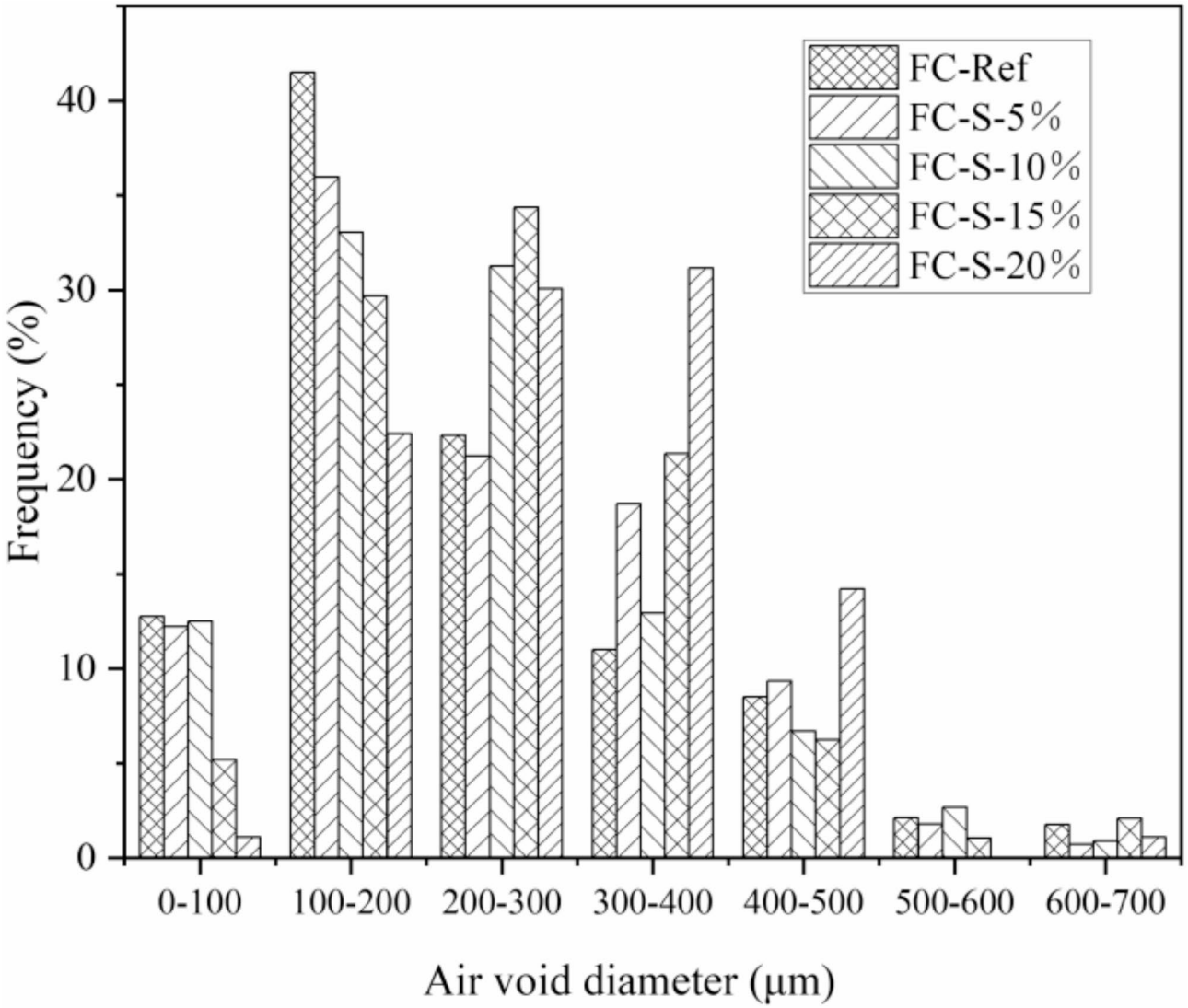

Fig. 7. The intricate web of pores within foamed concrete and their distribution patterns.

With the increase in GT contents, the content of AFt and C-S-H can be increased. In the initial stages, the clinker within the binders undergoes hydration, resulting in the generation of CH. Subsequently, the quartz present in the gold mine tailings dissolves in the liquid phase and combines with the aforementioned CH to form a diverse array of CSH gels. Simultaneously, the pozzolanic activity of the quartz within the composition is activated, triggering a secondary hydration reaction that consumes the CH. Consequently, there is a notable increase in the quantities of C-S-H gels and C-A-S-H gels. Furthermore, the C3A present in the clinker can react with gypsum and water, resulting in the formation of ettringite (AFt) through the chemical activation of activators within the binders. Therefore, the proper content of GT in foamed concrete can increase the compressive strength[41]. However, the excessive mixing of gold tailings can lead to the gradual reduction of $Ca(OH)_2$ crystals which may result in an increase in internal pores and a deterioration in structural integrity, bring about a macroscopic decrease in compressive strength[42].

Conclusion

In a comprehensive exploration of the potential of gold tailings (GT) to augment the properties of foamed concrete, GT was utilized in the production of foam concrete. The principal findings can be summarized as follows:

1. The incorporation of GT leads to an augmentation of pore size in the pore structure, accompanied by a reduction in the uniformity of the pore structure.
2. The compressive strength of foamed concrete can be significantly improved by the judicious incorporation of an appropriate quantity of GT.
3. The denser and less porous microstructure resulting from the addition of GT may underlie the observed increase in compressive strength of the foamed concrete.

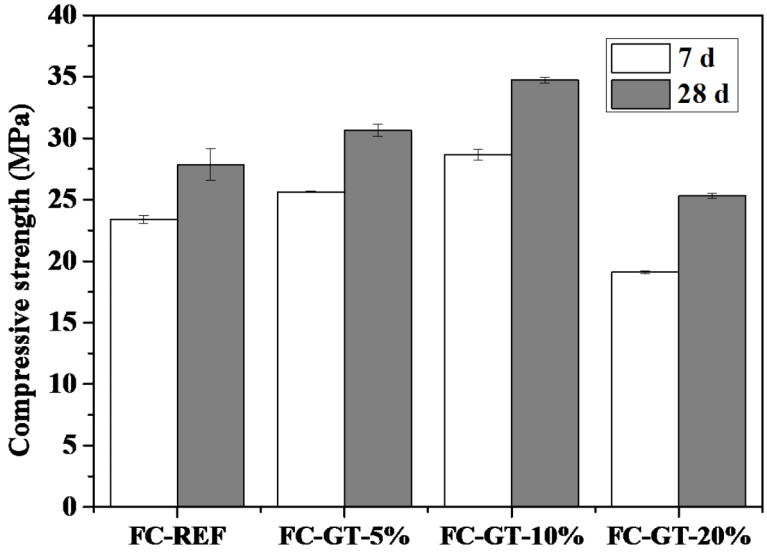

Fig. 8. Compressive strength of matrix with different dosage of GT.

Foamed concrete	Dry density of foamed concrete (kg/m^3)	Dry density of matrix (kg/m^3)	Density ratio	Experimental results (MPa)	Calculated results (MPa)	Relative deviation(%)
FC-REF	641	1430	0.448	1.94	2.02	4.1
FC-GT-5%	643	1447	0.441	2.02	2.08	3.0
FC-GT-10%	624	1411	0.442	2.19	2.37	8.2
FC-GT-20%	631	1405	0.449	1.70	1.86	9.4

Table 4. The compressive strength of both the experimental and calculated results.

4. Excessive admixture of GT can precipitate a gradual decline of $Ca(OH)_2$ crystals, potentially leading to an escalation in internal pores and a deterioration in structural integrity, ultimately manifesting as a discernible reduction in compressive strength.

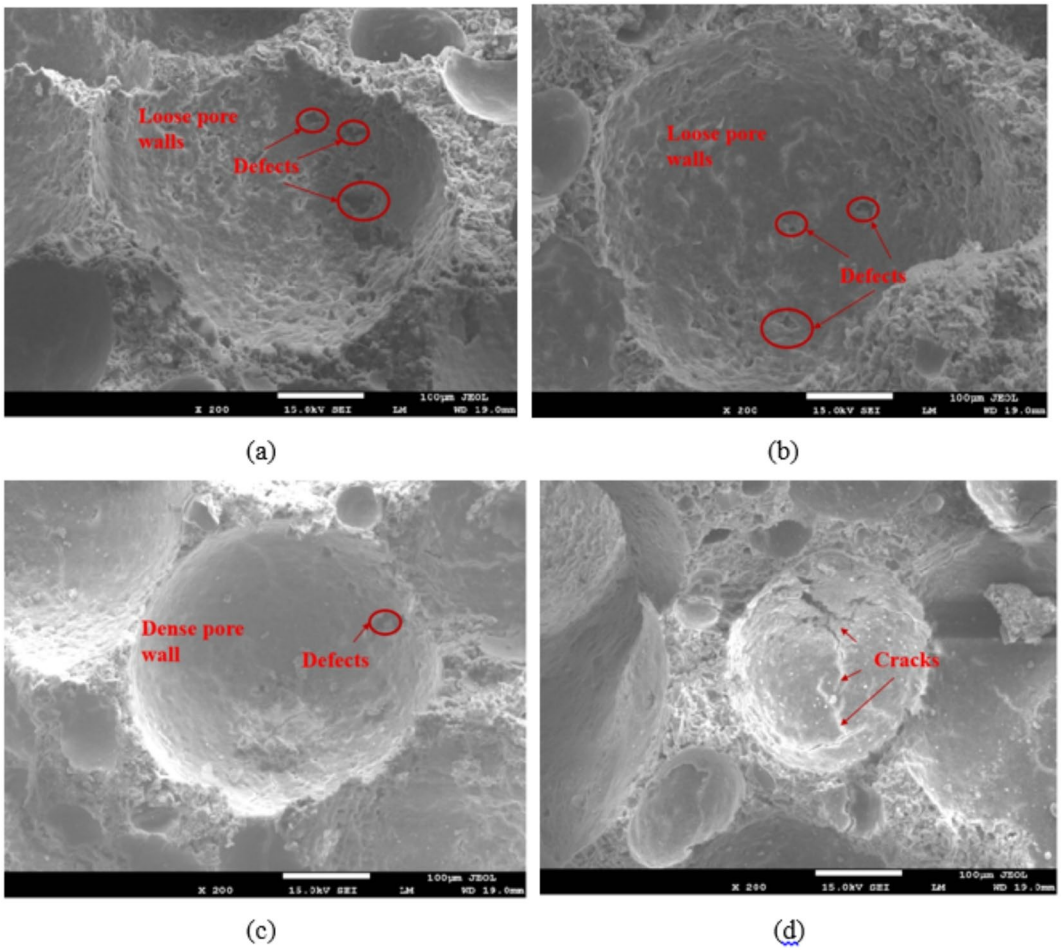

Fig. 9. Microstructures of foamed concrete with different dosage of GT. (**a**) FC-REF, (**b**) FC-GT-5%, (**c**) FC-GT-10%, (**d**) FC-GT-20%.

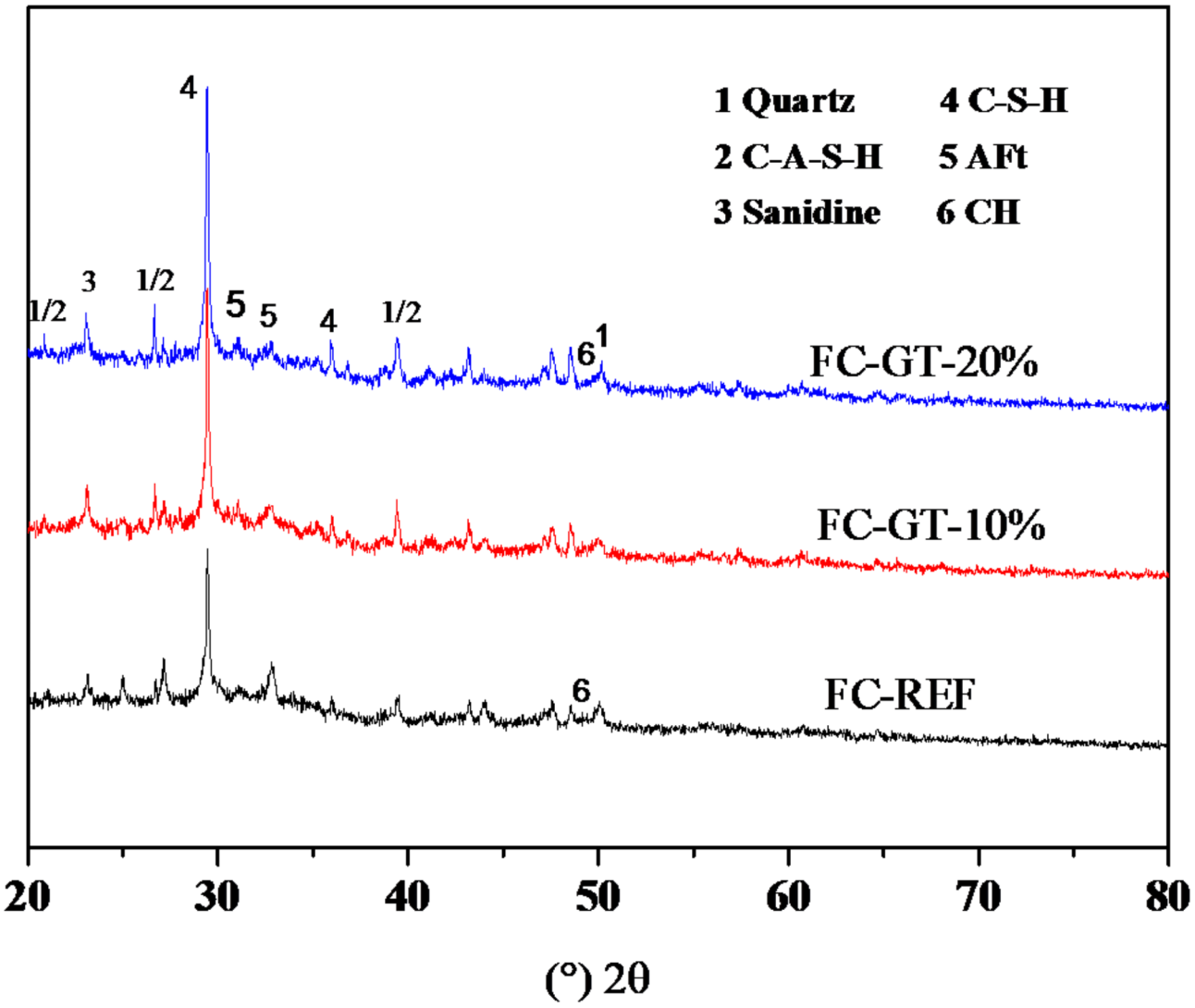

Fig. 10. XRD patterns of foamed concrete.

Data availability

The datasets used and/or analysed during the current study available from the corresponding author on reasonable request.

Received: 21 October 2024; Accepted: 28 January 2025
Published online: 12 February 2025

References

1. Hajimohammadi, A., Ngo, T. & Mendis, P. Enhancing the strength of pre-made foams for foamed applications. *Cem. Concr. Compos.* **87**, 164–171 (2018).
2. Chica, L. & Alzate, A. Cellular concrete review: New trends for application in construction. *Constr. Build. Mater.* **200**, 637–647 (2019).
3. Tran, N. P., Nguyen, T. N., Ngo, T. D., Le, P. K. & Le, T. A. Strategic progress in foam stabilisation towards high-performance foam concrete for building sustainability: A state-of-the-art review. *J. Clean. Prod.* **375**, 133939 (2022).
4. Alghamdi, H. & Neithalath, N. Synthesis and characterization of 3D-printable geopolymeric foams for thermally efficient building envelope materials. *Cem. Concr. Compos.* **104**, 103377 (2019).
5. Kaewmee, P., Song, M., Iwanami, M., Tsutsumi, H. & Takahashi, F. Porous and reusable potassium-activated geopolymer adsorbent with high compressive strength fabricated from coal fly ash wastes. *J. Clean. Prod.* **272**, 122617 (2020).
6. Kou, R. et al. Sound-insulation and photocatalytic foamed concrete prepared with dredged sediment. *J. Clean. Prod.* **356**, 131902 (2022).
7. Yang, F. et al. Preparation of environmentally friendly and energy-saving autoclaved aerated concrete using gold tailings. *J. N. Mater. Electrochem. Syst.* **22**(3), 159–64 (2019).
8. Wang, H. J. W. Y. J. et al. National mineral resources conservation and comprehensive utilization report. *China Land Resour. Econ.* **33**(2), 2 (2019).

9. Wang, P. et al. Leaching of heavy metals from abandoned mine tailings brought by precipitation and the associated environmental impact. *Sci. Total Environ.* **695**, 133893 (2019).
10. Huang, Z. et al. Leaching characteristics of heavy metals in tailings and their simultaneous immobilization with triethylenetetramine functioned montmorillonite (TETA-Mt) against simulated acid rain. *Environ. Pollut.* **266**, 115236 (2020).
11. Hu, Y. et al. Strength investigation and prediction of superfine tailings cemented paste backfill based on experiments and intelligent. *Methods. Mater.* **16**(11), 3995 (2023).
12. Shuaijun, C. et al. Formation mechanism and deformation characteristics of stratified cemented tailings backfill under noncontinuous filling system. *Constr. Build Mater.* **389**, 131623 (2023).
13. Zhang, Y. et al. Utilization of iron ore tailings with high volume in green concrete. *J. Build. Eng.* **72**, 106585 (2023).
14. Bing, Z., Yannian, Z. & Wenliang, L. Effect of iron tailing powder-based ternary admixture on acid corrosion resistance of concrete. *Materials* **16**(10), 3688 (2023).
15. Li, R., Yin, Z. & Hang, L. Research status and prospects for the utilization of lead–zinc tailings as building materials. *Buildings* **13**(1), 150 (2023).
16. Burduhos Nergis, D. D., Vizureanu, P., Sandu, A. V., Burduhos Nergis, D. P. & Bejinariu, C. XRD and TG-DTA study of new phosphate-based geopolymers with coal ash or metakaolin as aluminosilicate source and mine tailings addition. *Materials* **15**, 202. https://doi.org/10.3390/ma15010202 (2022).
17. Tahir, M. F. M. et al. Mechanical and durability analysis of fly ash based geopolymer with various compositions for rigid pavement applications. *Materials* **15**, 3458 (2022).
18. Aziz, I. H. et al. Recent developments in steelmaking industry and potential alkali activated based steel waste: A comprehensive review. *Materials* **1948**, 15 (2022).
19. Alieh, S. et al. Mechanical activation of lead–zinc mine tailings as a substitution for cement in concrete construction. *Construct. Build. Mater.* **364**, 129–973 (2023).
20. Celik, O., Elbeyli, I. Y. & Piskin, S. Utilization of gold tailings as an additive in Portland cement. *Waste Manag. Res.* **24**, 215–224 (2006).
21. Ahmed, T. et al. Development of ECO-UHPC utilizing gold mine tailings as quartz sand alternative. *Clean. Eng. Technol.* **4**, 100176 (2021).
22. Liang, Q. et al. Properties of lightweight foamed concrete containing gold tailings as subgrade filler. *Struct. Concrete* **66**, 1–18 (2024).
23. Xiong, Y., Zhu, Y., Chen, C. & Zhang, Y. Effect of nano-alumina modified foaming agents on properties of foamed concrete. *Constr. Build. Mater.* **267**, 121045 (2020).
24. Xiong, Y., Zhang, C., Chen, C. & Zhang, Y. Effect of superabsorbent polymer on the foam-stability of foamed concrete. *Cem. Concr. Compos.* **127**, 104398 (2022).
25. Xiong, Y., Li, B., Chen, C. & Zhang, Y. Properties of foamed concrete with $Ca(OH)_2$ as foam stabilizer. *Cem. Concr. Compos.* **118**, 103985 (2021).
26. Dhasindrakrishna, K., Pasupathy, K., Ramakrishnan, S. & Sanjayan, J. Effect of yield stress development on the foam-stability of aerated geopolymer concrete. *Cem. Concr. Res.* **138**, 106233 (2020).
27. Xiong, Y. et al. Effect of formic acid as an accelerator on foam-stability, compressive strength, and pore size distribution of foam concrete. *J. Build. Eng.* **66**, 105923 (2023).
28. Roussel, N., Stefani, C. & Leroy, R. From mini-cone test to Abrams cone test: Measurement of cement-based materials yield stress using slump tests. *Cem. Concr. Res.* **35**(5), 817–822 (2005).
29. Suh, J. I., Yum, W. S., Jeong, Y., Park, H. G. & Oh, J. E. The cation-dependent effects of formate salt additives on the strength and microstructure of CaO-activated fly ash binders. *Constr. Build. Mater.* **194**, 92–101 (2019).
30. Scrivener, K. L., Füllmann, T., Gallucci, E., Walenta, G. & Bermejo, E. Quantitative study of Portland cement hydration by X-ray diffraction/Rietveld analysis and independent methods. *Cem. Concr. Res.* **34**, 1541–1547 (2004).
31. Jansen, D., Goetz-Neunhoeffer, F., Stabler, C. & Neubauer, J. A remastered external standard method applied to the quantification of early OPC hydration. *Cem. Concr. Res.* **41**, 602–608 (2011).
32. Ramamurthy, K., Nambiar, E. K. K. & Ranjani, G. I. S. A classification of studies on properties of foam concrete. *Cem. Concr. Compos.* **31**(6), 388–396 (2009).
33. Bai, C. & Colombo, P. Processing, properties and applications of highly porous geopolymers: A review. *Ceram. Int.* **44**(14), 16103–16118 (2018).
34. Feneuil, B., Roussel, N. & Pitois, O. Optimal cement paste yield stress for the production of stable cement foams. *Cem. Concr. Res.* **120**, 142–151 (2019).
35. Eugénie, S. P., Fabrice, D., Gérard, C. & Samir, M. Effect of bulk viscosity and surface tension kinetics on structure of foam generated at the pilot scale. *Food Hydrocolloid.* **34**, 104–111 (2014).
36. Jones, M. R., Ozlutas, K. & Zheng, L. Stability and instability of foamed concrete. *Mag. Concr. Res.* **68**, 542–549 (2016).
37. Yaseen, Z. M. et al. Predicting compressive strength of lightweight foamed concrete using extreme learning machine model. *Adv. Eng. Softw.* **115**, 112–125 (2018).
38. Kearsley, E. & Wainwright, P. The effect of high fly ash content on the compressive strength of foamed concrete. *Cem Concr Res.* **31**, 105–112 (2001).
39. Kearsley, E. & Wainwright, P. The effect of porosity on the strength of foamed concrete. *Cem. Concr. Res.* **32**, 233–239 (2002).
40. Xue, L., Zhang, Z., Liu, H., Jiang, Y. & Wang, H. Drying shrinkage behavior of hybrid alkali activated cement (HAAC) mortars. *Constr. Build. Mater.* **316**, 126068 (2022).
41. Li, J. et al. Fabrication of baking-free bricks using gold tailings and cemented materials with low alkalinity. *J. Renew. Mater.* **27**(11), 3041–3058 (2022).
42. Wang, Z. et al. Influence of carlin-type gold mine tailings addition on the synthesis temperature, alkali-resistant performance, and hydration mechanism of Portland cement. *Constr. Build. Mater.* **359**, 129458 (2022).

Acknowledgements

The authors gratefully acknowledge the financial support from the "Natural Science Foundation of Shandong Province (grant number ZR2023QE264)" and "Shandong Province Transportation Technology Plan Project (TTKJ2023-15)".

Author contributions

Wang Xinyu: Conceptualization, Methodology, Validation, Formal analysis, Data curation, Investigation, Writing-original draft, Visualization, Software. Xiong Yuanliang: Resources, Writing-review & editing, Supervision, Project administration. Zhang Chunfei: Methodology, Validation, Formal analysis, Data curation. Wang Yuanjing: Supervision, Formal analysis, Data curation. Liu Bo: Resources, Writing-review & editing, Supervision, Project administration. Liu Yuming: Methodology, Validation, Formal analysis, Data curation.

Declarations

Competing interests
The authors declare no competing interests.

Additional information
Correspondence and requests for materials should be addressed to B.L.

Reprints and permissions information is available at www.nature.com/reprints.

Publisher's note Springer Nature remains neutral with regard to jurisdictional claims in published maps and institutional affiliations.